

Successive phase transitions under high pressure in FeTe_{0.92}

Hironari OKADA^{1,4*}, Hiroyuki TAKAHASHI¹, Yoshikazu MIZUGUCHI^{2,3,4}, Yoshihiko TAKANO^{2,3,4}, and Hiroki TAKAHASHI^{1,4}

¹*Department of Physics, College of Humanities and Sciences, Nihon University, Sakurajosui, Setagaya-ku, Tokyo 156-8550, Japan*

²*National Institute for Materials Science, 1-2-1, Sengen, Tsukuba, 305-0047, Japan*

³*University of Tsukuba, 1-1-1, Tennodai, Tsukuba, 305-8577, Japan*

⁴*JST, Transformative Research-Project on Iron Pnictides (TRIP), 5 Sanbancho, Chiyoda, Tokyo 102-0075, Japan*

(Received)

We performed the electrical resistivity measurements under high pressures up to 19 GPa for FeTe_{0.92}. The compound shows an anomaly in the resistivity at atmospheric pressure due to a structural distortion accompanied by a magnetic transition. We found appearances of two resistive anomalies under high pressure, suggesting that two pressure-induced phase transitions occur. Unlike FeAs-based compounds, superconductivity was not detected under high pressures up to 19 GPa, although the resistive anomaly at atmospheric pressure was suppressed by applying pressure. The existence of high pressure phases may inhibit the emergence of superconductivity in FeTe_{0.92}.

KEYWORDS: iron-based superconductor, FeTe, high pressure, electrical resistivity, superconductivity

Soon after the discovery of FeAs-based superconductors with superconducting transition temperature T_c of up to 55 K,¹⁻⁵⁾ superconductivity with $T_c = 8$ K in tetragonal FeSe_x was discovered.⁶⁾ Similar to FeAs-based superconductors, the tetragonal FeSe_x has edge-sharing FeSe₄ layers and the crystal structure is composed of a stack of Fe₂Se₂ layers along the *c*-axis. The T_c of FeSe_x is increased by the substitution of Se by S and Te.⁷⁻⁹⁾ In contrast to FeSe_x, isostructural Fe_{1+x}Te does not show superconductivity, but exhibits a first-order structural phase transition accompanied by an antiferromagnetic (AFM) transition.^{10,11)} Depending on the amount of excess Fe, *x*, Fe_{1+x}Te has different crystal and magnetic structures at low temperature despite the same tetragonal structure at room temperature. The compound with nearly stoichiometric composition exhibits a monoclinic distortion and a commensurate AFM ordering at low temperature, whereas an orthorhombic and an incommensurate AFM structures are realized in the composition with large amount of excess Fe. The incommensurate AFM ordering locks into the commensurate AFM ordering with decreasing excess Fe. Although the structural distortion and the magnetic structures at low temperature are different from those observed for FeAs-based compounds,¹²⁻¹⁶⁾ the structural and magnetic phase transitions are suppressed by the substitution of Te by S and Se, like FeAs-based compounds, and then superconducting transition with $T_c = 10-14$ K occurs.^{7,8,17-20)}

Superconductivity in FeAs-based compounds is very sensitive to external pressure. Not only the substitution effect, but external pressure also affects appearance of superconductivity in parent compounds of FeAs-based superconductors, which results from the suppression of structural phase transition from tetragonal to orthorhombic and AFM ordering by applying pressure.²¹⁻²⁵⁾ Superconductivity of FeSe_x is also sensitive to external pressure and shows a huge enhancement of the T_c , which reaches up to 37 K at 7-9 GPa.²⁶⁻²⁸⁾ This pressure effect of FeSe_x is larger than that of LaFeAsO_{1-x}F_x.²⁹⁾ A previous work on high pressure study of FeTe_{0.92} reveals that a resistive anomaly due to the structural and magnetic phase transitions tends to be suppressed by applying pressure, although the applied pressure is limited up to 1.6 GPa.³⁰⁾ In addition, theoretical investigation on stoichiometric FeS, FeSe and FeTe predicts that the Fermi surface of these compounds is very similar to that of FeAs-based compounds and both FeSe and FeTe show spin density wave ground state.³¹⁾ The instability of spin density wave in FeTe is stronger than that of FeSe. Therefore, it is expected that superconductivity with higher T_c than FeSe_x is realized under higher pressure region in FeTe. In this study, we performed electrical resistivity measurements under high pressure up to 19 GPa for FeTe_{0.92}. We could not detect a signature of pressure-induced superconductivity, but found pressure-induced successive phase transitions in FeTe_{0.92}.

Single crystal with nominal composition $\text{FeTe}_{0.92}$ was grown using a melting method. Polycrystalline $\text{FeTe}_{0.92}$ sample,³⁰⁾ which is the starting material for single crystals, was sealed into an evacuated quartz tube with an alumina crucible. The sample was heated at 1123 K and slowly cooled to 1053 K with a rate of 1 K/hour. Electrical resistivity along in-plane direction under high pressure is measured by a standard dc four-probe technique. Pressures of up to 2.5 GPa were applied using a piston-cylinder (CuBe/NiCrAl) type cell. A liquid pressure-transmitting medium (Daphne 7474) was used to maintain hydrostatic condition.³²⁾ The applied pressure was estimated from T_c of lead manometer. A diamond anvil cell (DAC) was used for electrical resistivity measurements under high pressures up to 19 GPa. The sample chamber comprising a stainless steel gasket was filled with powdered NaCl as a pressure-transmitting medium. Fine ruby powders scattered in the sample chamber was used to determine the applied pressure by means of a standard ruby fluorescence method.

Figure 1 shows the temperature dependences of electrical resistivity $\rho(T)$ below 160 K at various pressures up to 2.5 GPa, using the piston-cylinder type pressure cell. The data at 0, 0.4, 1.1, 1.3 and 1.6 GPa are shifted upward by 3.5, 3.2, 2.5, 1.5 and 0.5 $\mu\Omega\text{m}$, respectively. The $\rho(T)$ at 0 GPa slightly increases with decreasing temperature and shows a sudden decrease at $T_s = 69$ K. Below T_s , it rapidly decreases with decreasing temperature. The $\rho(T)$ at 0 GPa is similar to that of Fe_{1-x}Te with nearly stoichiometric composition rather than that of large excess Fe composition having a semiconductive behavior in $\rho(T)$.^{7,10,19)} Therefore, it is considered that the sudden decrease at T_s is due to the monoclinic distortion and the commensurate AFM ordering. By applying pressure, the T_s shifts to lower temperature, and we observed another anomaly at $T_1 = 62$ K at 1.1 GPa. The T_1 slightly decreases with increasing pressure, whereas the anomaly at T_s was not detected at 1.6 GPa. By further applying pressure, in addition to the anomaly at T_1 , we found that $\rho(T)$ at 1.8 GPa shows a large drop at $T_2 = 45$ K. The T_2 increases with increasing pressure, while the T_1 is not detected above 2.3 GPa.

Figure 2 shows the pressure dependence of the electrical resistivity at 4.2 and 200 K. The resistivity at 200 K monotonically decreases with increasing pressure. On the other hand, the resistivity at 4.2 K increases in the vicinity of 1.6 GPa, which corresponds to the appearance of the anomaly at T_1 , and then rapidly decreases above ~ 2.0 GPa. The $\rho(T)$ data below the characteristic temperatures T_s , T_1 and T_2 show different curves. For instance, the $\rho(T)$ below T_1 is relatively gradual temperature dependence compared with those of below T_s and T_2 . These results suggest that two pressure-induced phase transitions occur at T_1 and T_2 , and that

the band structure and/or the scattering mechanism change due to the phase transition, resulting in the different $\rho(T)$ curves below T_s , T_1 and T_2 .

The pressure dependence of the characteristic temperatures T_s , T_1 and T_2 observed by the electrical resistivity measurements under high pressures up to 2.5 GPa is shown in Fig. 3. The T_s , T_1 and T_2 were determined by the temperature at which $d\rho/dT$ shows maximum, indicated in Fig. 1 by arrows. The T_s decreases with increasing pressure, which is consistent with results of polycrystalline sample in previous report.³⁰⁾ However, in our measurement using single crystals, we observed that the T_s vanishes at ~ 1.5 GPa, indicating the disappearance of the monoclinic and AFM phase observed at 0 GPa. In addition, the first high pressure phase below T_1 appears at ~ 1.0 GPa above T_s , and the second high pressure phase below T_2 is induced above ~ 1.8 GPa. The T_s and T_2 are sensitive to external pressure, whereas the pressure dependence of T_1 is quite small. Particularly, the T_2 rises steeply with pressure at a rate of ~ 37 K/GPa, indicating that the high pressure phase below T_2 is rapidly stable to higher temperatures at high pressures. It is worth noting that, at 1.6 GPa, the phase transition at T_1 occurs but the transitions at T_s and T_2 are not detected.

Figure 4 shows the temperature dependence of the electrical resistivity under high pressures up to 19 GPa, using the DAC. A rapid decrease, which corresponds to the anomaly of the electrical resistivity at T_2 , was also observed in this measurement. We could not estimate the T_2 in this measurement because of the broadening of the anomaly due to a nonhydrostatic compressive stress arising from the use of a solid pressure-transmitting medium. However, we can see that the rapid decrease of the $\rho(T)$ steeply shifts to higher temperature with increasing pressure and reaches up to above 300 K at 10 GPa. This result is consistent with the results using the piston cylinder type cell. By further applying pressure above 10 GPa, the $\rho(T)$ shows a negative temperature coefficient at lower temperature. The origin of this behavior is unclear at present, but it may suggest that further pressure-induced transition occurs above 10 GPa. In our measurements, no sign of pressure-induced superconductivity was detected even in high pressures up to 19 GPa.

From the recent reports of FeAs-based compounds,²¹⁻²⁵⁾ the parent compounds have an antiferromagnetically ordered orthorhombic phase at low temperature, and superconductivity is induced by suppression of both the orthorhombic structure and the antiferromagnetic state through substitution and/or pressure effects. Although the low temperature phase at 0 GPa of FeTe_{0.92} was suppressed by pressure, we could not observe signature of pressure-induced superconductivity. Instead, we found two resistive anomalies under high pressure, suggesting

that pressure-induced phase transitions occur above ~ 1.0 GPa. Pressure-induced phase transition has also been reported in CaFe_2As_2 , which is a member of FeAs-based compounds having a ThCr_2Si_2 -type tetragonal structure. CaFe_2As_2 exhibits a structural phase transition from a tetragonal to the orthorhombic phase at 0 GPa.¹⁵⁾ The compound also has a nonmagnetic collapsed tetragonal phase above ~ 0.35 GPa, which shows a drastic reduction of 9.5 % of the c -lattice parameter and 11% of the c/a ratio in comparison with the orthorhombic phase.^{33,34)} The collapsed tetragonal phase is caused by an enhancement of As-As bonds between neighboring FeAs layers under high pressure.³⁵⁾ The crystal structure of $\text{FeTe}_{0.92}$ has a simple crystal structure only composed of a stack of FeTe layers along c -axis. Moreover, recent X-ray diffraction experiments under high pressure for FeSe reveals that the compound shows the smallest bulk modulus of ~ 30 GPa and the largest compressibility along the c -axis among FeAs-based compounds.^{27,28,36)} In addition, the magnetic structure of Fe_{1+x}Te is sensitive to atomic substitution and deviation of stoichiometric composition.^{10,11)} Therefore, it is expected that $\text{FeTe}_{0.92}$ also have small bulk modulus and large anisotropic compression, and that the Te-Te hybridization between neighboring FeTe layers is enhanced by applying pressure, leading to structural and magnetic phase transitions under high pressure. In the view of the tetragonal structures of FeTe and CaFe_2As_2 , the atomic position of neighboring Te atoms between neighboring FeTe layers is different from that in CaFe_2As_2 . In case of CaFe_2As_2 having the ThCr_2Si_2 -type structure with the tetragonal space group $I4/mmm$, the As atoms are occupied at $4e$ $(0,0,z)$ site and the neighboring As atoms between FeAs layers are located along the c -axis. Hence, the enhancement of As-As bonds causes the reduction of the c -lattice parameter without changing the symmetry. On the other hand, FeTe has a α -PbO type structure with a tetragonal space group $P4/nmm$ and the Te atoms are occupied at the $2c$ $(1/4,1/4,z)$ site. Considering this difference of the atomic position, the enhancement of the Te-Te hybridization may induces different structural distortion and magnetic transition from those in CaFe_2As_2 , resulting in the unique P - T phase diagram as shown in Fig. 3.

In summary, we performed electrical resistivity measurements under high pressures up to 19 GPa for $\text{FeTe}_{0.92}$. The resistive anomaly at $T_s = 69$ K at 0 GPa was suppressed by applying pressure. However, we could not detect pressure-induced superconductivity up to 19 GPa. Instead, we found that two resistive anomalies at T_1 and T_2 appear at 1.1 and 1.8 GPa, respectively. The obtained results suggest that $\text{FeTe}_{0.92}$ has two high pressure phases and the existence of the high pressure phases inhibit the emergence of superconductivity under high pressure. In order to clarify the origin of the high pressure phases, further high pressure studies for $\text{FeTe}_{0.92}$ are now in progress.

Acknowledgment

This work was supported by Grant-in-Aid for Young Scientists (Start-up), JST-TRIP and Nihon University Research Grant for 2009.

References

- 1) Y. Kamihara, T. Watanabe, M. Hirano, and H. Hosono: *J. Am. Chem. Soc.* **130** (2008) 3296.
- 2) X. H. Chen, T. Wu, G. Wu, R. H. Liu, H. Chen, and D. F. Fang, *Nature* **453** (2008) 761.
- 3) C. F. Chen, Z. Li, D. Wu, G. Li, W. Z. Hu, J. Dong, P. Zheng, J. L. Luo, and N. L. Wang: *Phys. Rev. Lett.* **100** (2008) 247002.
- 4) Z. A. Ren, G. C. Che, X. L. Dong, J. Yang, W. Lu, W. Yi, X. L. Shen, Z. C. Li, L. L. Sun, F. Zhou, and Z. X. Zhao: *Europhys. Lett.* **83** (2008) 17002.
- 5) M. Rotter, M. Tegel, and D. Johrendt: *Phys. Rev. Lett.* **101** (2008) 107006.
- 6) F. C. Hsu, J. Y. Luo, K. W. Yeh, T. K. Chen, T. W. Huang, P. M. Wu, Y. C. Lee, Y. L. Huang, Y. Y. Chu, D. C. Yan, and M. K. Wu: *Proc. Natl. Acad. Sci. U.S.A* **105** (2008) 14262.
- 7) M. H. Fang, H. M. Pham, B. Qian, T. J. Liu, E. K. Vehstedt, Y. Liu, L. Spinu, and Z. Q. Mao: *Phys. Rev. B* **78** (2008) 224503.
- 8) K. W. Yeh, T. W. Huang, Y. L. Huang, T. K. Chen, F. C. Hsu, P. M. Wu, Y. C. Lee, Y. Y. Chu, C. L. Chen, J. Y. Luo, D. C. Yan, and M. K. Wu: *Europhys. Lett.* **84** (2008) 37002.
- 9) Y. Mizuguchi, F. Tomioka, S. Tsuda, T. Yamaguchi, and Y. Takano: arXiv:0811.1123.
- 10) W. Bao, Y. Qiu, Q. Huang, M. A. Green, P. Zajdel, M. R. Fitzsimmons, M. Zhernenkov, M. Fang, B. Qian, E. K. Vehstedt, J. Yang, H. M. Pham, L. Spinu, and Z. Q. Mao: arXiv:0809.2058.
- 11) S. Li, C. de la Cruz, Q. Huang, Y. Chen, J. W. Lynn, J. Hu, Y. L. Huang, F. C. Hsu, K. W. Yeh, M. K. Wu, and P. Dai: *Phys. Rev. B* **79** (2009) 054503.
- 12) C. de la Cruz, Q. Huang, J. W. Lynn, J. Li, W. Ratcliff II, J. L. Zarestky, H. A. Mook, G. F. Chen, J. L. Luo, N. L. Wang, and P. Dai: *Nature* **453** (2008) 899.
- 13) T. Nomura, S. W. Kim, Y. Kamihara, M. Hirano, P. V. Sushko, K. Kato, M. Takata, A. L. Shluger, and H. Hosono: *Supercond. Sci. Technol.* **21** (2008) 125028.
- 14) Q. Huang, Y. Qiu, W. Bao, M. A. Green, J. W. Lynn, Y. C. Gasparovic, T. Wu, G. Wu, and X. H. Chen: *Phys. Rev. Lett.* **101** (2008) 257003.
- 15) N. Ni, S. Nandi, A. Kreyssig, A. I. Goldman, E. D. Mun, S. L. Bud'ko, and P. C. Canfield: *Phys. Rev. B* **78** (2008) 014523.
- 16) J. Q. Yan, A. Kreyssig, S. Nandi, N. Ni, S. L. Bud'ko, A. Kracher, R. J. McQueeney, R. W. McCallum, T. A. Lograsso, A. I. Goldman, and P. C. Canfield: **78** (2008) 024516.
- 17) Y. Mizuguchi, F. Tomioka, S. Tsuda, T. Yamaguchi, and Y. Takano: *Appl. Phys. Lett.* **94** (2009) 012503.

- 18) B. C. Sales, A. S. Sefat, M. A. McGuire, R. Y. Jin, and D. Mandrus: *Phys. Rev. B* **79** (2009) 094521.
- 19) G. F. Chen, Z. G. Chen, J. Dong, W. Z. Hu, G. Li, X. D. Zhang, P. Zheng, J. L. Luo, and N. L. Wang: arXiv:0811.1489
- 20) M. H. Fang, B. Qian, H. M. Pham, J. H. Yang, T. J. Liu, E. K. Vehstedt, L. Spinu, and Z. Q. Mao: arXiv:0811.3021.
- 21) M. S. Torikachvili, S. L. Bud'ko, N. Ni, and P. C. Canfield: *Phys. Rev. Lett.* **101** (2008) 057006.
- 22) T. Park, E. Park, H. Lee, T. Klimczuk, E. D. Bauer, F. Ronning, and J. D. Thompson: *J. Phys.: Condens. Matter* **20** (2008) 322204.
- 23) P. L. Alireza, Y. T. Chris Ko, J. Gillett, C. M. Petrone, J. M. Cole, G. G. Lonzarich, and S. E. Sebastian: *J. Phys.: Condens. Matter* **21** (2009) 012208.
- 24) H. Kotegawa, H. Sugawara, and H. Tou: *J. Phys. Soc. Jpn.* **78** (2009) 013709.
- 25) H. Okada, K. Igawa, H. Takahashi, Y. Kamihara, M. Hirano, H. Hosono, K. Matsubayashi, and Y. Uwatoko: *J. Phys. Soc. Jpn.* **77** (2008) 113712.
- 26) Y. Mizuguchi, F. Tomioka, S. Tsuda, T. Yamaguchi, and Y. Takano: *Appl. Phys. Lett.* **93** (2008) 152505.
- 27) S. Margadonna, Y. Takabayashi, Y. Ohishi, Y. Mizuguchi, Y. Takano, T. Kagayama, T. Nakagawa, M. Takata, and K. Prassides: arXiv:0903.2204.
- 28) S. Medvedev, T. M. McQueen, I. Trojan, T. Palasyuk, M. I. Erements, R. J. Cava, S. Naghavi, F. Casper, V. Ksenofontov, G. Wortmann, and C. Felser: arXiv:0903.2143.
- 29) H. Takahashi, K. Igawa, K. Arii, Y. Kamihara, M. Hirano, and H. Hosono: *Nature* **453** (2008) 376.
- 30) Y. Mizuguchi, F. Tomioka, S. Tsuda, T. Yamaguchi, and Y. Takano: arXiv:0810.5191.
- 31) A. Subedi, L. Zhang, D. J. Singh, and M. H. Du: *Phys. Rev. B* **78** (2008) 134514.
- 32) K. Murata, K. Yokogawa, H. Yoshino, S. Klotz, P. Munsch, A. Irizawa, M. Nishiyama, K. Iizuka, T. Nanba, T. Okada, Y. Shiraga, and S. Aoyama: *Rev. Sci. Instrum.* **79** (2008) 085101.
- 33) A. Kreyssig, M. A. Green, Y. Lee, G. D. Samolyuk, P. Zajdel, J. W. Lynn, S. L. Bud'ko, M. S. Torikachvili, N. Ni, S. Nandi, J. B. Leão, S. J. Poulton, D. N. Argyriou, B. N. Harmon, R. J. McQueeney, P. C. Canfield, and A. I. Goldman: *Phys. Rev. B* **78** (2008) 184517.
- 34) A. I. Goldman, A. Kreyssig, K. Prokeš, D. K. Pratt, D. N. Argyriou, J. W. Lynn, S. Nandi, S. A. J. Kimber, Y. Chen, Y. B. Lee, G. Samolyuk, J. B. Leão, S. J. Poulton, S. L. Bud'ko, N. Ni, P. C. Canfield, B. N. Harmon, and R. J. McQueeney: *Phys. Rev. B* **79** (2009)

024513.

35) T. Yildirim: Phys. Rev. Lett. **102** (2009) 037003.

36) J. N. Millican, D. Phelan, E. L. Thomas, J. B. Leão, and E. Carpenter: Solid State Commun. **147** (2009) 707.

Figure captions

Fig. 1. (Color Online) Temperature dependence of the electrical resistivity under various pressures up to 2.5 GPa, using the piston cylinder type cell. The data at 0, 0.4, 1.1, 1.3 and 1.6 GPa are shifted upward by 3.5, 3.2, 2.5, 1.5 and 0.5 $\mu\Omega\text{m}$, respectively. The arrows indicate the characteristic temperature T_s , T_1 and T_2 determined by the temperature at which the $d\rho/dT$ shows maximum.

Fig. 2. (Color Online) Electrical resistivity at 4.2 and 200 K as a function of pressure.

Fig. 3. (Color Online) Pressure dependence of the characteristic temperatures T_s , T_1 and T_2 .

Fig. 4. (Color Online) Temperature dependence of the resistance under various pressures up to 19 GPa, using the DAC.

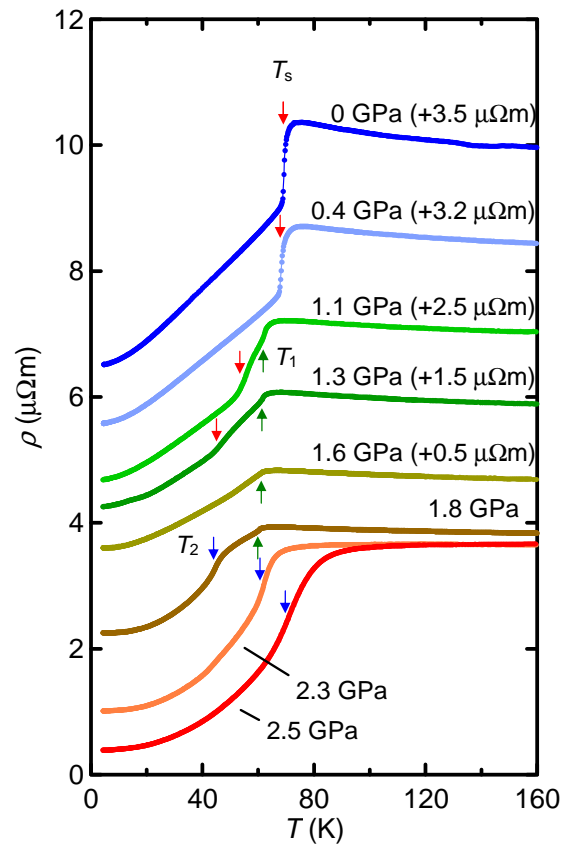


Fig. 1
H. Okada *et al.*

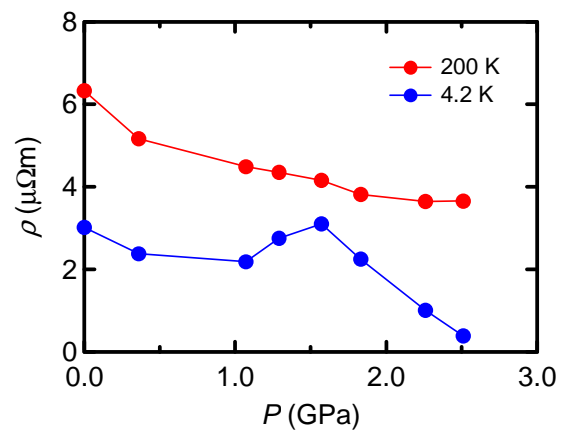


Fig. 2
H. Okada *et al.*

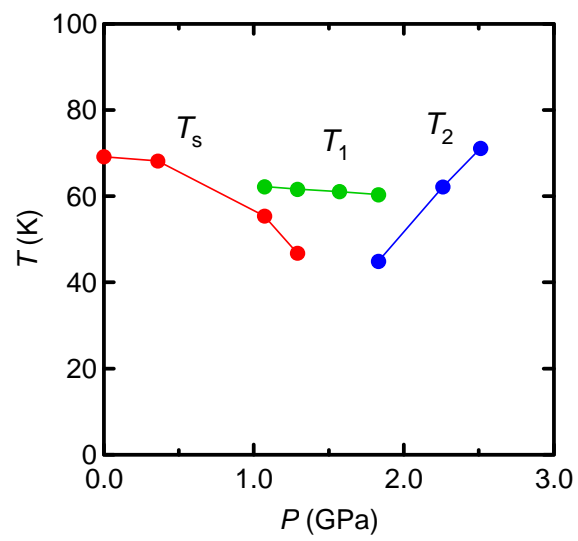


Fig. 3
H. Okada *et al.*

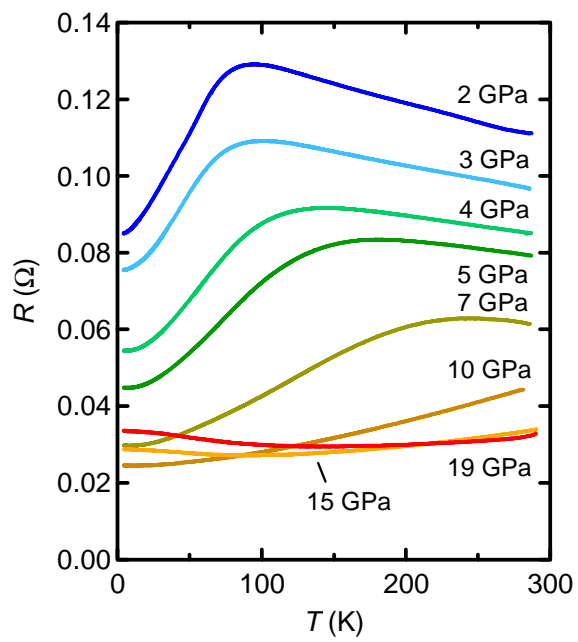


Fig. 4
H. Okada *et al.*